

THE DETERMINATION OF THE RESOLUTION OF THE  
VIRGINIA POLYTECHNIC INSTITUTE  
ELECTROSTATIC ACCELERATOR

by

John Howard Denny, Jr.

Thesis submitted to the Graduate Faculty of the  
Virginia Polytechnic Institute  
in candidacy for the degree of  
MASTER OF SCIENCE  
in  
Physics

APPROVED:

Director of Graduate Studies

Dean of Academic Science and  
Business Administration

APPROVED:

Head of Department

Supervisor or Major  
Professor

May, 1958

Blacksburg, Virginia

## TABLE OF CONTENTS

	<u>Page</u>
LIST OF TABLES. . . . .	4
LIST OF FIGURES . . . . .	5
INTRODUCTION. . . . .	6
DESCRIPTION OF ACCELERATOR. . . . .	7
THEORY OF OPERATION . . . . .	9
General Principles . . . . .	9
Spray Voltage Power Supply . . . . .	11
Ion Source . . . . .	14
Focus Control. . . . .	15
Resistor Cascade . . . . .	16
Analyzing Magnet . . . . .	17
Stabilization System . . . . .	17
CONTROL AND INSTRUMENTATION . . . . .	25
Vacuum Tube Microammeters. . . . .	25
Magnet Current . . . . .	29
Vacuum Detection . . . . .	29
Scintillation Detector . . . . .	30
Current Integrator . . . . .	32
ACCELERATOR OPERATING PROCEDURE . . . . .	36
EXPERIMENTAL PROCEDURE. . . . .	42
Method . . . . .	43
Results . . . . .	44
DISCUSSION OF RESULTS . . . . .	48
SUMMARY . . . . .	49

Table of Contents (con't)

	<u>Page</u>
ACKNOWLEDGMENTS . . . . .	50
BIBLIOGRAPHY. . . . .	51
VITA. . . . .	52

## LIST OF TABLES

<u>Tables</u>	<u>Page</u>
1. Calibration of Electronic Current Integrator . . . . .	34
2. Relative Yield as a Function of Magnet Current. . . . .	45

## LIST OF FIGURES

<u>Figures</u>	<u>Page</u>
1. Simplified Schematic of Accelerator . . . . .	10
2. Schematic Diagram of Spray Voltage Power Supply. . . . .	12
3. Schematic Diagram of Stabilizer D.C. Amplifier Power Supply. . . . .	20
4. Static Plate Characteristics of 4-125A Stabilizer . . . . .	22
5. Schematic Diagram of Modified Stabilizer. . . . .	23
6. Schematic Diagram of Vacuum Tube Microammeter. . . . .	26
7. Schematic Diagram of Scintillation Detector. . . . .	31
8. Calibration of Electronic Current Integrator. . . . .	35
9. Relative Yield Vs. Magnet Current . . . . .	46
10. Differential Spectrum . . . . .	47

## INTRODUCTION

The Virginia Polytechnic Institute's Van de Graaff accelerator was designed and constructed by the Physics Department under the direction of Dr. T. M. Hahn, Jr. Although at present it is a proton accelerator its design is such that it can be converted to an electron accelerator with only minor changes. At present it is capable of accelerating protons to an energy of 2 Mev and future plans call for an increase to 4 Mev.

This thesis describes the design and construction of many of the electronic control and instrumentation devices, the modification of previous projects, and a determination of the resolution of the completed accelerator.

## DESCRIPTION OF ACCELERATOR

In this electrostatic accelerator, an aluminum dome with a radius of 12 inches is raised to any positive potential between approximately 200 kilovolts and two million volts. This potential is then used for the acceleration of protons. The proton source and control circuits are mounted inside the aluminum terminal, the entire terminal system being supported horizontally by three textolite tubes. The high voltage terminal is charged positively as a result of its losing electrons to a positively charged belt. The charging belt, 92 inches long and six inches wide, is made of neoprene rubber and is driven by a three horsepower, 220 volt, three-phase motor. The belt, motor and pulleys were obtained from the High Voltage Engineering Corp. of Cambridge, Mass.

The protons produced in the ion source inside the high voltage terminal are accelerated by the dome potential through the accelerating tube, analyzing magnet, and slit box to the target. The accelerating tube is composed of 32 cylindrical sections of ceramic. The ceramic sections are separated by aluminum electrodes and bonded together under pressure with vinyl plastic, forming a column strong enough to be self-supporting from one end.

During machine operation, the high voltage terminal,

accelerating tube, and belt mechanism are pressurized in a steel cylinder approximately four feet in diameter and eight feet in length, which is mounted on wheels and a track for easy removal. The system is pressurized in an inert atmosphere of 80% nitrogen and 20% carbon dioxide to a pressure of 10 atmospheres. The gas is dried by a Lectrodryer type BAC dryer to a dew point of at least  $-40^{\circ}$  C and compressed by an Engersol type 30 compressor.

The entire proton path from ion source to target is evacuated to a pressure of approximately  $5.0 \times 10^{-6}$  mm of mercury by a Consolidated Vacuum Co. type MCF-300 oil-diffusion pump and MB-100 booster pump.

With the exception of the gas handling system, the entire accelerator can be controlled from a remote control room.



## THEORY OF OPERATION

General Principles

The two fundamental physical principles on which the operation of a Van de Graaff type accelerator is based are the following: the limiting potential to which a given insulated, hollow conductor can be charged by internal contact is determined only by the insulation of its supports. The potential inside such a hollow conductor is zero. The first of these two principles is used in electrostatic generators to develop potentials of the order of several million volts. The second principle is utilized in the production and control of charged particles inside the highly charged body. The charged particles can then be ejected from the charged body and accelerated by the large potential to energies sufficient for the penetration of the atomic nucleus.

The general principles of operation can be seen in Fig. 1 which is a simplified schematic of the accelerator. The belt is driven by a motor connected to the lower pulley. The lower pulley, which is insulated from ground, is maintained at a large negative potential by the spray power supply. This potential forces electrons from the belt by corona discharge to the lower spray points, leaving the belt positively charged. The positively charged belt

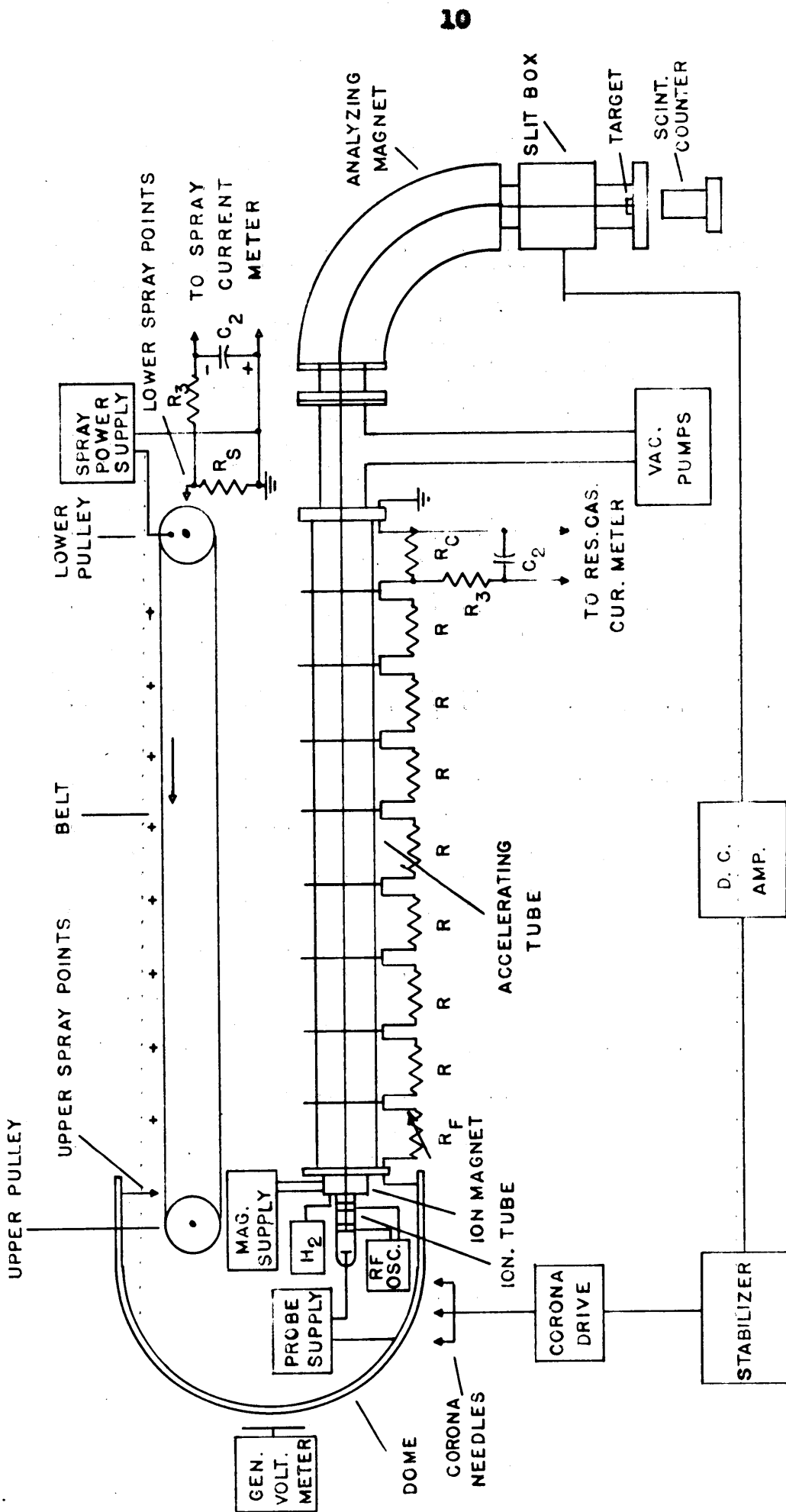


FIG. 1 SIMPLIFIED SCHEMATIC OF ACCELERATOR

is neutralized by attracting electrons from the dome through the upper spray points, thus leaving the dome positively charged. Potentials of several million volts can be obtained in this manner in a few seconds.

Power for the production and control of the accelerating particles is furnished by a generator built into the upper pulley. This generator produces 120 volts A.C. and has a power rating of 550 watts.

Protons are formed in the ionization tube by the ionization of the hydrogen gas which is stored under pressure in the dome. The protons are then forced from the ionization tube by the probe power supply and then accelerated by the potential of the dome through the evacuated accelerating tube, analyzing magnet, and slit box to the target.

#### Spray Voltage Power Supply

The output voltage from the spray power supply can be varied from zero to 25,000 volts, the desired output voltage being obtained by varying the input voltage to a high voltage transformer with a variac. This control is located on the console in the control room. A schematic of this power supply is shown in Fig. 2. The belt drive switch  $S_1$ , filament switch  $S_2$ , and plate supply switch  $S_3$  are connected in series to eliminate the

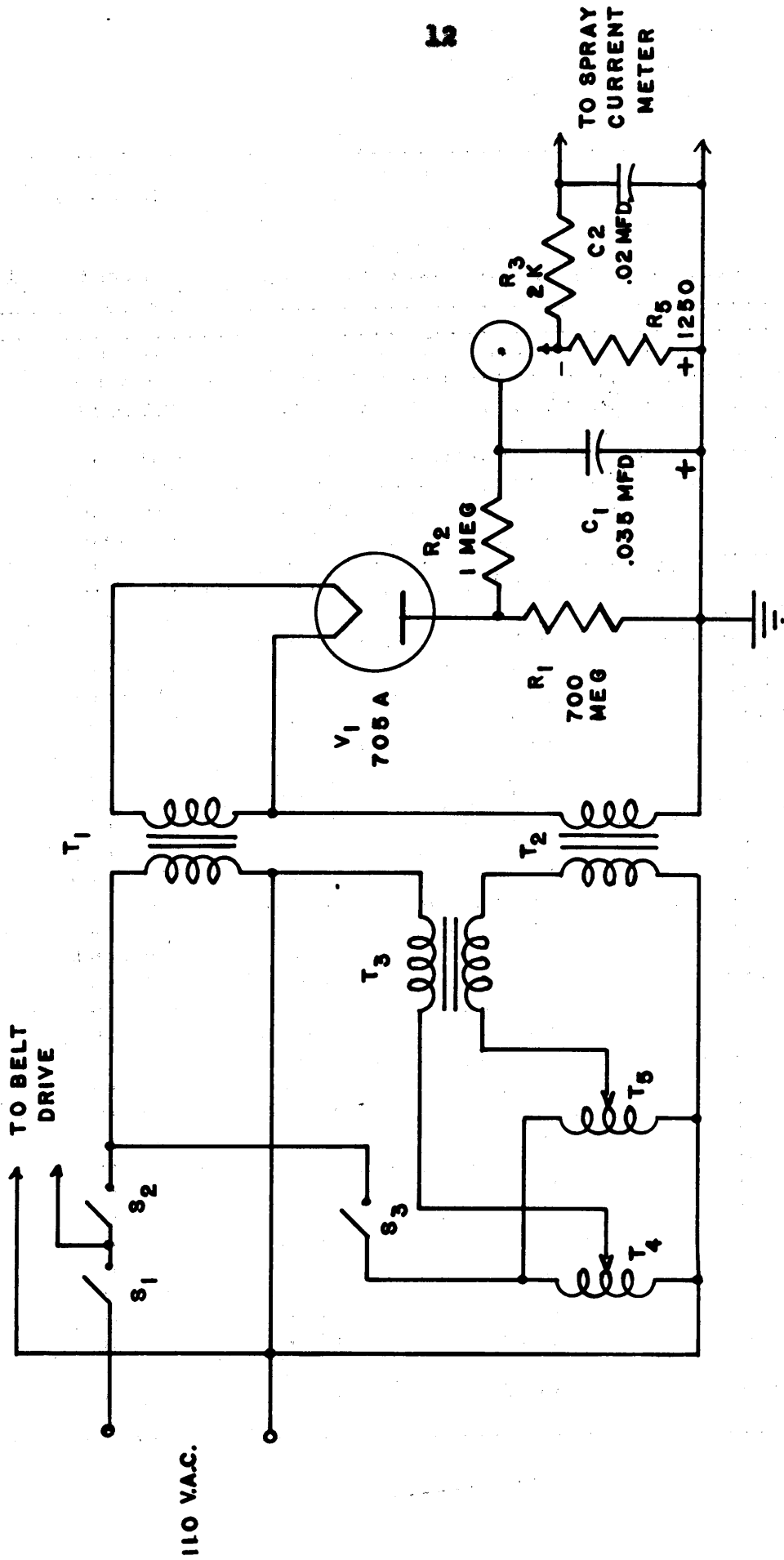


FIG.2 SCHEMATIC OF SPRAY POWER SUPPLY

possibility of applying spray voltage when the belt is stationary. Therefore, the plate voltage of the 705A tube cannot be applied without first starting the belt and then closing the filament switch. Closing the plate supply switch should be delayed at least 30 seconds after closing the filament switch to prevent possible damage to the tube cathode surface that would result from the application of the plate voltage before the filament had reached operating temperature. Resistor  $R_2$  and capacitor  $C_1$  form a low-pass filter, reducing the 60-cycle ripple from the half-wave rectifier supply by a factor of approximately 15 and reducing the D.C. output a maximum of only 400 volts under the maximum belt-charging current of 400 microamperes. Variac  $T_4$  and transformer  $T_3$  form a vernier control for the spray voltage by superimposing a small voltage, which is variable from zero to 2.5 volts, on the input voltage to the plate transformer  $T_2$ . This small change in input voltage to  $T_2$  results in a very precise control of the spray voltage, providing a variation of zero to 625 volts in the spray voltage. Capacitor  $C_1$  is a General Electric pyronol capacitor rated at 50,000 volts. Resistor  $R_5$  is a spray current metering resistor, selected to give a full scale deflection on the spray current meter when the spray current is 400 microamperes.

### Ion Source

The protons that are accelerated by the high potential of the dome are formed inside the dome, the action being remotely controlled with selsyn motors located on the control room console and on an auxiliary unit located beside the machine. As shown in Fig. 1, hydrogen gas is stored under pressure in a pressure vessel inside the dome. The flow of gas into the ionization tube is regulated by a palladium leak. This device consists of a thimble of palladium metal surrounded by a heating coil. The hydrogen gas cannot penetrate the crystalline structure when the metal is at room temperature, however, when the palladium is heated by the coil, the crystalline structure expands and the hydrogen can diffuse into the ionization tube. The heating is controlled by a variac which is adjusted remotely with a selsyn motor.

Initial ionization is produced by a 100 watt radio-frequency oscillator operating at approximately 100 mc/sec and connected between the two connectors shown on the ionization tube in Fig. 1. The ionization is made more efficient by the ionization magnet which has an axial magnetic field. This field causes the protons to follow a spiral trajectory when moving under the influence of the probe voltage. The increased path-length yields

more protons by increasing the probability of collision between the protons and the hydrogen molecules. The spiral path also eliminates the tendency of the protons to diffuse by mutual repulsion to the outside of the ionization tube.<sup>1</sup>

The protons formed in the ionization tube are expelled into the accelerating tube by the probe power supply. This supply, whose output voltage is variable from zero to 6,000 volts by a variac driven by a selsyn motor, maintains a positive potential between the electrode in the end of the ionization tube and the dome. Thus the electrode is at a higher potential than the dome and the protons can be expelled into the accelerating tube where they are accelerated by the potential of the dome. Complete details of the ionization process and the associated control circuits have been reported previously.<sup>9</sup>

### Focus Control

The divergent stream of protons expelled from the dome into the accelerating tube is formed into a beam and focused at the focal point of the analyzing magnet by varying the potential difference between the dome and the first electrode of the accelerating tube. The potential difference is determined by a variable resistor,  $R_f$  in Fig. 1, which is connected between the dome and the

focus electrode. The focus is adjusted remotely by a selsyn motor. There is some interaction between the focus control and the probe voltage control, and in operation the optimum setting is determined by the sharpness of the beam as viewed on the quartz disk inside the first viewing section.

### Resistor Cascade

The resistor cascade is composed of 32 S.S. White type 80X resistors, each having a resistance of 700 megohms. The purpose of these resistors is to form a potential gradient down the accelerating tube that does not exceed the breakdown potential of the individual sections of the tube. The potential of each electrode is made uniform across the machine by a circular ring made of 3/8 inch aluminum tubing formed in a circle of 12 inches radius and placed perpendicular to the accelerating tube and electrically connected to the electrodes. The last resistor in the resistor cascade,  $R_c$  in Fig. 1, is the metering resistor for the current. Its resistance was chosen to give a full-scale deflection of the Resistor Cascade Current meter when 100 microamperes of current flows. Since this current is that flowing through the series resistors when the potential of the dome is at



its maximum of 2 million volts, this meter gives an indication of the dome potential.

### Analyzing Magnet

The beam that reaches the analyzing magnet is a polyenergetic beam of protons. The analyzing magnet is a momentum filter and allows particles of only one given energy to be transmitted, so the beam emerging from the magnet is monoenergetic. The magnet is water cooled, of the circumferential yoke type with a 16 inch radius, and provides a 90 degree beam deflection. Double focusing provides maximum beam intensity at the target and the field intensity of 10,000 gauss is sufficient for analyzing the proposed 4 Mev deuteron beam. The magnet is energized by an electronically regulated motor-generator set that provides a magnet current that is stable to within  $\pm 0.01\%$ . Complete details of the magnetic analyzer and its control system are given in Oliver<sup>8</sup> and Chramic.<sup>3</sup>

### Stabilization System

The beam emerging from the analyzing magnet passes through the slit box. The slit box, shown schematically in Fig. 1, is a part of the beam stabilizing system which includes in addition to the slit box, a balanced D.C. amplifier, a corona needle drive, and a stabilizer which

is a 4-125A vacuum tube.

The slit box contains two adjustable jaws in both the vertical and horizontal directions, providing a means of adjusting the size of the beam impinging upon the target. The horizontal slits are insulated from ground but electrically returned to ground through a resistor. The potentials developed across these two resistors as a result of the interception of portions of the beam, are fed to the D.C. amplifier.

The D.C. amplifier has two inputs, one connected to each of the horizontal slit jaws. The two input signals are amplified in separate channels and then fed into a difference amplifier. When the beam energy is constant the two input signals are equal and there is no output from the difference amplifier, but when a change in beam energy occurs the two input signals are not equal and an error signal is developed. The D.C. amplifier also supplies the grid bias for the 4-125A stabilizer, the error signal being superimposed upon the bias voltage. This change in bias causes the stabilizer to draw a different current from the dome and thus return the dome potential to its original value.

In order to achieve finer control and more stable operation of the D.C. amplifier circuit, there have been several modifications made in its circuitry. Finer control has been achieved by replacing the bias potentiometer with

a ten-turn precision helipot. More stable operation has been achieved by replacing with two separate coax cables the multiple connector cable that carried both the ground corona current and the bias voltage. Excessive drift of the D.C. amplifier was eliminated with a regulated power supply.

As shown in the schematic in Fig. 3, the power supply consists of an electronically regulated output rated at + 210 volts with a current capacity of 60 milliamperes and a voltage-regulator tube supply rated at - 150 volts with a current capacity of 40 milliamperes. In the 210 volt supply tube  $V_3$  is the series control tube which regulates the output voltage. Voltage-regulator tube,  $V_5$ , is the reference source and holds the cathode of the error amplifier,  $V_4$ , at a constant potential. Since the cathode is held constant, an increase in output voltage decreases the grid bias of  $V_4$ . This change is amplified by  $V_4$  causing a decrease in its plate voltage. But since the control grid of  $V_3$  is connected directly to the plate of  $V_4$ , the grid bias on  $V_3$  increases. This increases its plate resistance and the voltage drop across the tube and corrects the original increase in output voltage.

The negative-voltage supply is a half-wave rectifier using a two section pi-filter as the filtering element and a VR-150 tube as the regulating element. Except for the

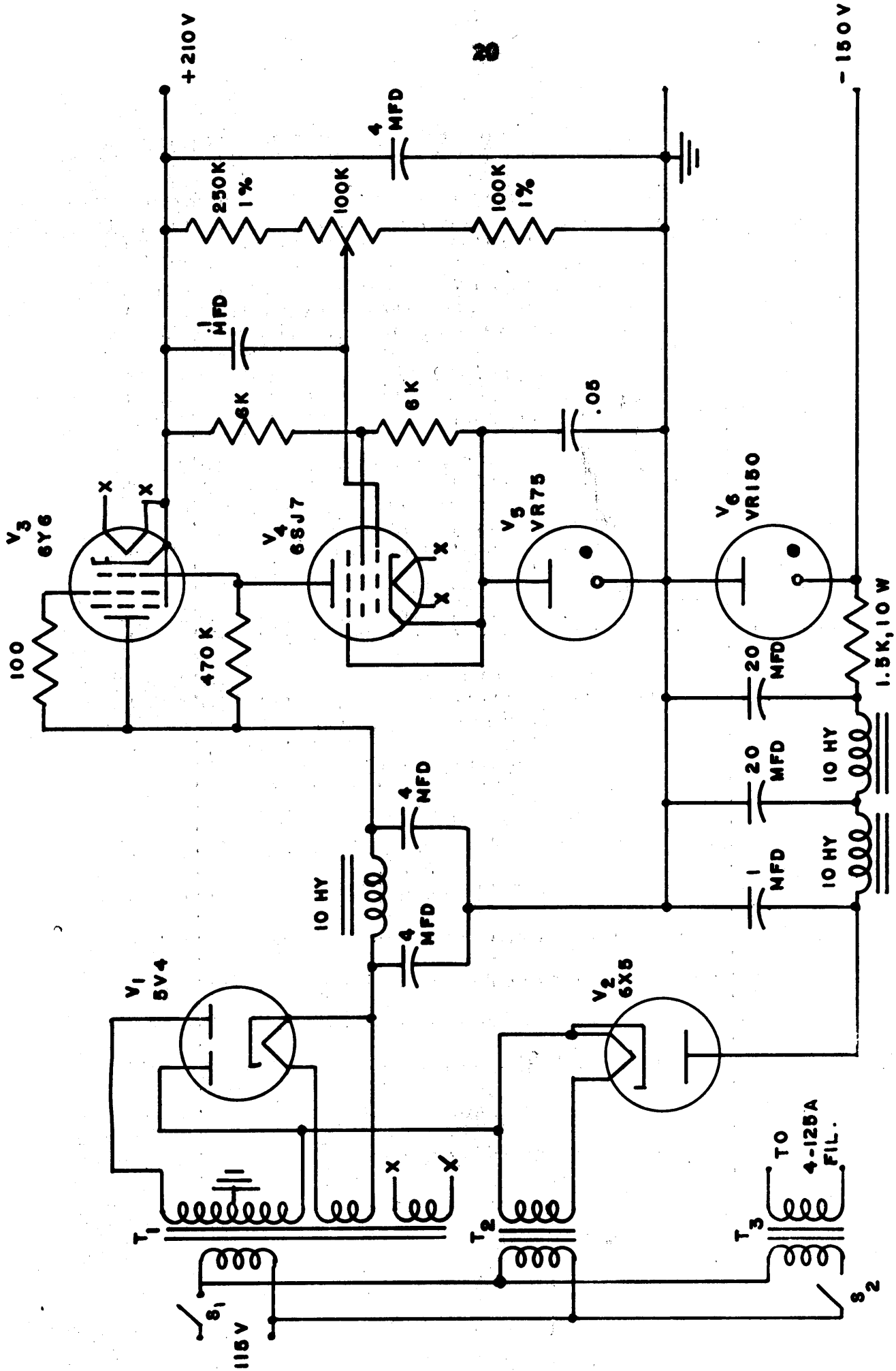


FIG 3 SCHEMATIC OF STABILIZER D.C. AMPLIFIER POWER SUPPLY

manner in which the high voltage for this supply is obtained, the supply is quite conventional. Obtaining the high voltage by tapping to one side of the positive supply transformer eliminated another power transformer, although it did necessitate filament transformer  $T_2$ . The polarity of the filter capacitors should be noted when replacements are necessary because a reversal of the polarities shown will short the entire supplies and destroy the filters.

Since the 4-125A tube used as the stabilizing element is operated with a plate current of 25 to 100 microamperes, published data for its characteristics in this range were not available. The static plate characteristics were obtained by a point-by-point plot of plate current versus plate voltage for various values of grid voltage with a constant screen voltage of 67.5 volts. The results are plotted in Fig. 4. The quiescent operating point for the stabilizer was chosen in the fairly linear portion of the characteristic represented by a plate voltage of 1600 volts and a grid bias of -22v. This results in a quiescent plate current of 70 microamperes.

The 4-125A stabilizer circuit has been modified to that shown in Fig. 5. Switch  $SW_1$  which is located on the D.C. amplifier front panel allows the circuit to be energized remotely from the control console. The cathode

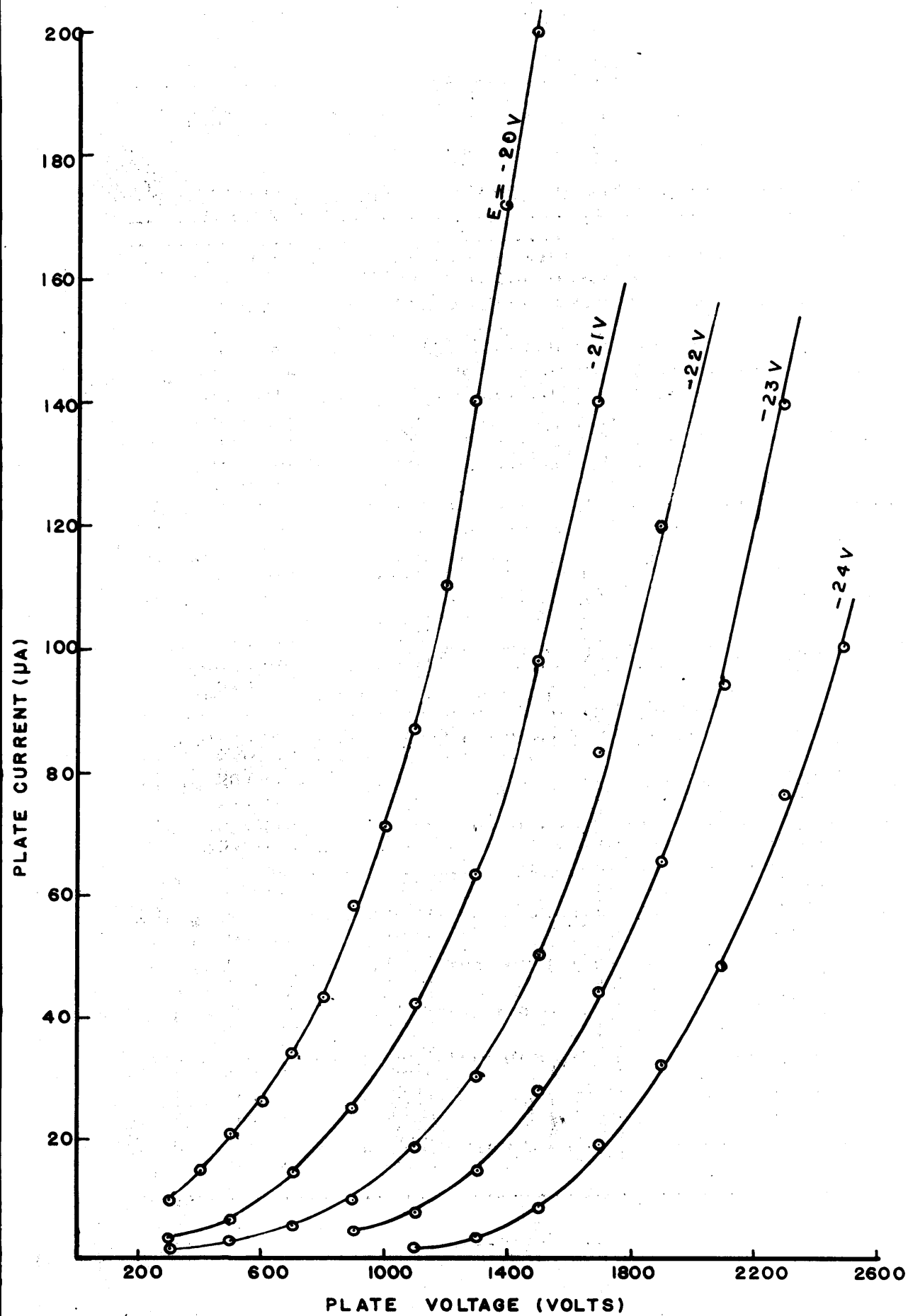


FIG. 4 STATIC PLATE CHARACTERISTICS OF 4-125A

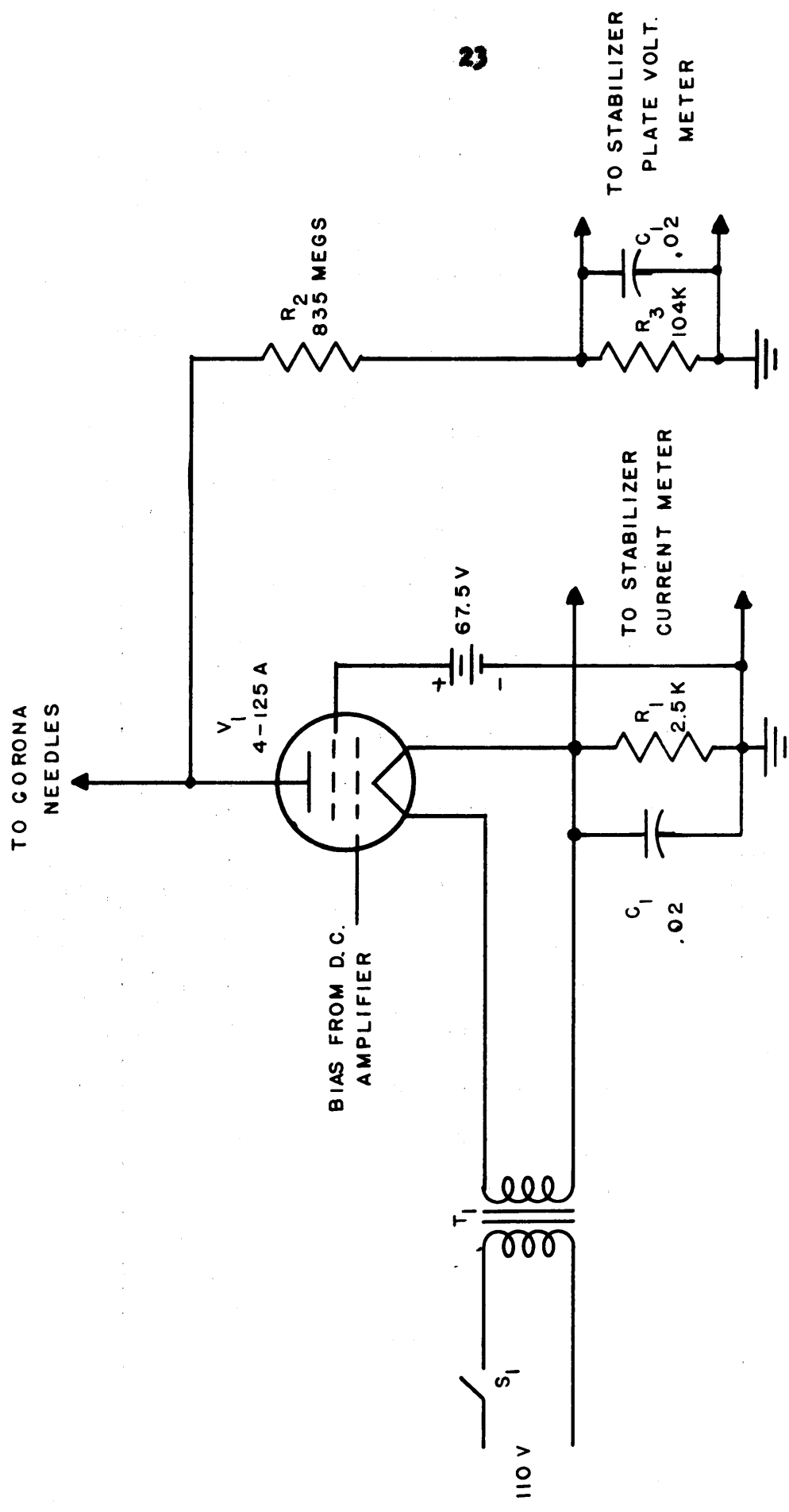


FIG. 5 SCHEMATIC OF MODIFIED STABILIZER

resistor  $R_1$  monitors the total cathode current while resistors  $R_2$  and  $R_3$  form a voltage divider circuit that permits monitoring of the plate voltage. The cathode current and plate voltage are displayed on the control room console since they determine the operating point of the automatic stabilizing circuit. The plate voltage for the circuit is supplied by the dome potential through the corona needles.

The corona needles can be positioned remotely from the console thus permitting the proper voltage to be applied to the stabilizer. If the corona needles are not properly adjusted, current may flow from the dome to the corona needles support. A microammeter is inserted between the corona needles support and ground to provide a constant check on this condition. The meter is located on the D.C. amplifier front panel and is labeled ground-corona current. Replacing the signal cable from the corona needles support to the remotely located meter with separate coaxial cable eliminated an oscillation in the stabilizer circuit.



## CONTROL AND INSTRUMENTATION

Vacuum Tube Microammeters

Conventional moving-coil meters cannot be used in electrostatic accelerators because frequent sparking destroys them. A solution to the problem is the use of vacuum tube meters in which the current flowing through the moving-coil meter is limited by the characteristics of the vacuum tube. One such circuit that has been used quite extensively<sup>5</sup> has been adapted to monitor all the remote current and voltage measurements necessary for the control of the accelerator. The schematic diagram of the microammeter is shown in Fig. 6 where the circuit has been drawn to emphasize the operation. The circuit is battery operated and is energized from the control console with switches  $S_1$  and  $S_2$  which are relay contacts. Tube  $V_1$  provides all the amplification of the input signal and the output current is registered on meter  $M_1$ . The cathode current of tube  $V_2$  flows through the meter in the opposite direction and is used to zero the meter deflection when there is no input signal. The current flowing in  $V_2$  is determined by the variable resistor  $R_2$ . Resistor  $R_2$  and the meter are located on the control console. Resistor  $R$  is determined by the application and is located externally. The meter is deflected

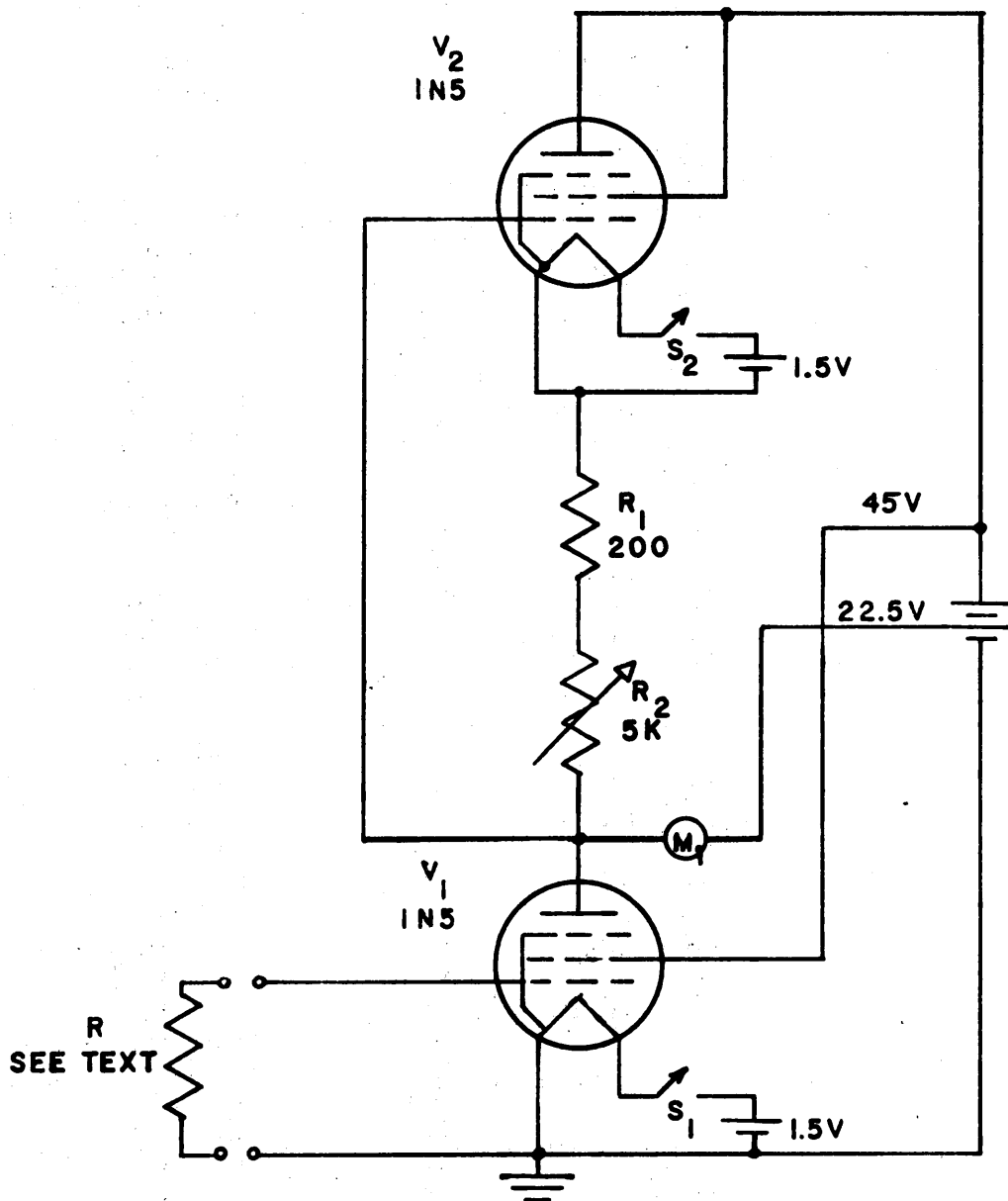


FIG. 6 SCHEMATIC OF VACUUM TUBE MICROAMMETER

full-scale when the input voltage developed across resistor R is 0.5 volts and the polarity of the grid is positive.

The stabilizer plate voltage meter circuit is that described above. Resistor R was calculated from the voltage divider connected, as shown in Fig. 5, from the plate of the tube to ground. The stabilizer circuit was designed to draw a maximum current from the dome of 100 microamperes and the voltage divider circuit was designed to draw 5 microamperes. Resistor R was calculated to give a full-scale deflection of the indicating meter at the maximum plate voltage of 3000 volts. A 0.02 microfarad capacitor was shunted across resistor R to eliminate the electrical noise caused by the corona to the needles.

The stabilizer cathode current meter circuit is also the basic microammeter. The function of resistor R and capacitor  $C_1$  is the same as above, resistor R being calculated to give a full-scale deflection of 200 microamperes.

The spray current meter circuit is the basic microammeter except for the ground point. As shown in Fig. 2, the voltage developed across the spray current metering resistor is negative with respect to the accelerator ground. The correct polarity for the circuit was obtained by grounding the grid of  $V_1$  to the accelerator ground

and connecting the signal lead to the B<sup>-</sup> of the battery. Resistor R was calculated to give a full-scale deflection on the indicating meter with a spray current of 400 microamperes. Resistor R<sub>3</sub> and capacitor C<sub>2</sub> form a low-pass filter that attenuates the high frequency components caused by the spray corona. Since the input circuit draws negligible grid current, there is no D.C. loss across R<sub>3</sub>.

The resistor cascade current meter circuit is also the basic microammeter. As shown in Fig. 1, this circuit measures the current in the series cascade of resistors connected between the dome and ground. Thus the dome potential can be calculated from the measured current and the known total resistance. In operation, however, this instrument is not used to give precise measurements of dome potential because the resistance of the cascade resistors changes somewhat with the temperature and humidity. Resistor R<sub>c</sub> which is the input resistor for the microammeter was calculated to give a full-scale deflection of 100 microamperes with a dome potential of two million volts. Thus the meter indicates the approximate voltage of the dome, full-scale representing two million volts. Resistor R<sub>3</sub> and capacitor C<sub>2</sub> form the same low-pass filter as described above for the spray current meter.

### Magnet Current

The primary reference for the determination of the energy of the particles is a standard resistor connected in series with the analyzing magnet. The current flowing through the magnet is determined by measuring, with a Leeds & Northrup potentiometer, the voltage drop across the standard resistor. Thus, a given beam energy may be selected by setting the potentiometer to the corresponding current as shown on the magnet calibration curves given in Carson.<sup>2</sup> Once the machine is stabilized at this energy it is possible to obtain any energy within several hundred thousand electron volts by adjusting only the potentiometer. The stabilizing system will automatically follow the potentiometer within this range.

### Vacuum Detection

In the pressure range down to  $10^{-3}$  mm of mercury, the vacuum is measured with a thermocouple gauge, the output of the thermocouple driving a Weston sensitrol relay and voltmeter. The diffusion pump heater relay and a warning bell are connected in series with the sensitrol relay. Thus, the diffusion pumps cannot be turned on until the fore pumps have reduced the pressure to  $10^{-3}$  mm of mercury. Also, the diffusion pumps are turned off and the warning bell sounded if the pressure rises to this

pre-determined level. In the range  $10^{-3}$  to  $10^{-8}$  mm of mercury, the vacuum is measured with a Consolidated Vacuum Company type DPA 38 ionization gauge.

### Scintillation Detector

The scintillation detector for the detection of gamma rays is shown schematically in Fig. 7. The photomultiplier tube is a Du Mont type 6292, which is a ten-stage multiplier of the end-window type. The circuit was designed for operation with 125 volts per stage, this being a compromise between stability, signal-to-noise ratio, and amplification. Resistor  $R_2$  is a variable resistor for adjusting the potential of the internal shield. This adjustment determines the optimum photoelectron collection efficiency. The exact voltage will vary from tube to tube but is usually several volts more positive than the cathode.

A sodium iodide crystal enclosed in a thin aluminum casing and surrounded by magnesium oxide was mounted directly on the end window of the photomultiplier tube and the entire assembly was mounted in a mu-metal magnetic shield. The high voltage was supplied by an Atomic Instrument Company Model 312 super-stable power supply. The negative output pulses were amplified with an Atomic type 219A preamplifier located near the target and further



amplified with an Atomic Model 218 linear amplifier and registered with an Atomic Model 210 single channel analyzer.

A series of tests with a constant source of radiation showed that the power supply required at least one hour of warm-up before reproducible results could be obtained with the scintillation detector.

### Current Integrator

A more useful quantity than the total number of gamma rays produced in any given reaction is the relative yield. The relative yield is a normalized quantity and is defined as the ratio of the total number of gamma rays produced to the number of incident particles. In practice a number proportional to the total number of incident particles is used in computing the relative yield.

The target, which is insulated from ground by several thousand megohms, develops a large positive potential when bombarded with the proton beam. This potential charges a low-leakage capacitor connected between the target mount and ground. Connected in parallel with the capacitor is some discharging device so that the energy stored in the capacitor can be discharged through a counting device when the potential reaches a predetermined value. Originally, the discharging device was similar



to the Watt<sup>11</sup> type integrator which consists of a neon bulb and a series resistor connected across the capacitor. Thus, when the potential across the capacitor reaches the firing potential of the neon bulb, the capacitor is discharged through the resistor. The resultant pulse developed across the resistor is used to actuate an electronic recorder. If the counter connected to the scintillation counter is started and stopped at the same instant as the current integrator counter, the relative yield can be determined from the resultant counts.

This passive-type integrator was found to have some undesirable non-linearities in its characteristics and has been replaced with an electronic type integrator similar in essential details to that shown in Elmore and Sands.<sup>4</sup>

The integrator was calibrated by allowing a known current to flow into the circuit and plotting the resulting output counts as a function of the input current. The current was measured with a Leeds & Northrup galvanometer having a sensitivity of 0.0051 microamperes per millimeter of deflection. The voltage was supplied by a highly regulated power supply and the output pulses were recorded with an Atomic Instrument Company glow tube scaler. The results are tabulated in Table 1 and

plotted in Fig. 8. The data was taken after allowing two hours warm up time for thermal equilibrium. The excellent linearity shows the advantage of the electronic type integrator.

Table 1. CALIBRATION OF CURRENT INTEGRATOR

Galvanometer Deflection (mm.)	Input Current ( $\mu$ A)	Total Counts	Count Time (min.)	Counts/min.
8.0	0.041	456	2	228
9.0	0.046	420	1	420
10.0	0.051	630	1	630
12.0	0.061	1406	1	1406
14.0	0.072	2090	1	2090
16.0	0.082	2705	1	2705
18.0	0.092	3403	1	3403
20.0	0.102	4013	1	4013
22.0	0.112	4627	1	4627
24.0	0.122	5301	1	5301
26.0	0.133	6029	1	6029
28.0	0.143	6670	1	6670
30.0	0.153	7237	1	7237
32.0	0.164	7940	1	7940
34.0	0.174	8596	1	8596
36.0	0.184	9205	1	9205
38.0	0.194	9784	1	9784
40.0	0.204	10405	1	10405

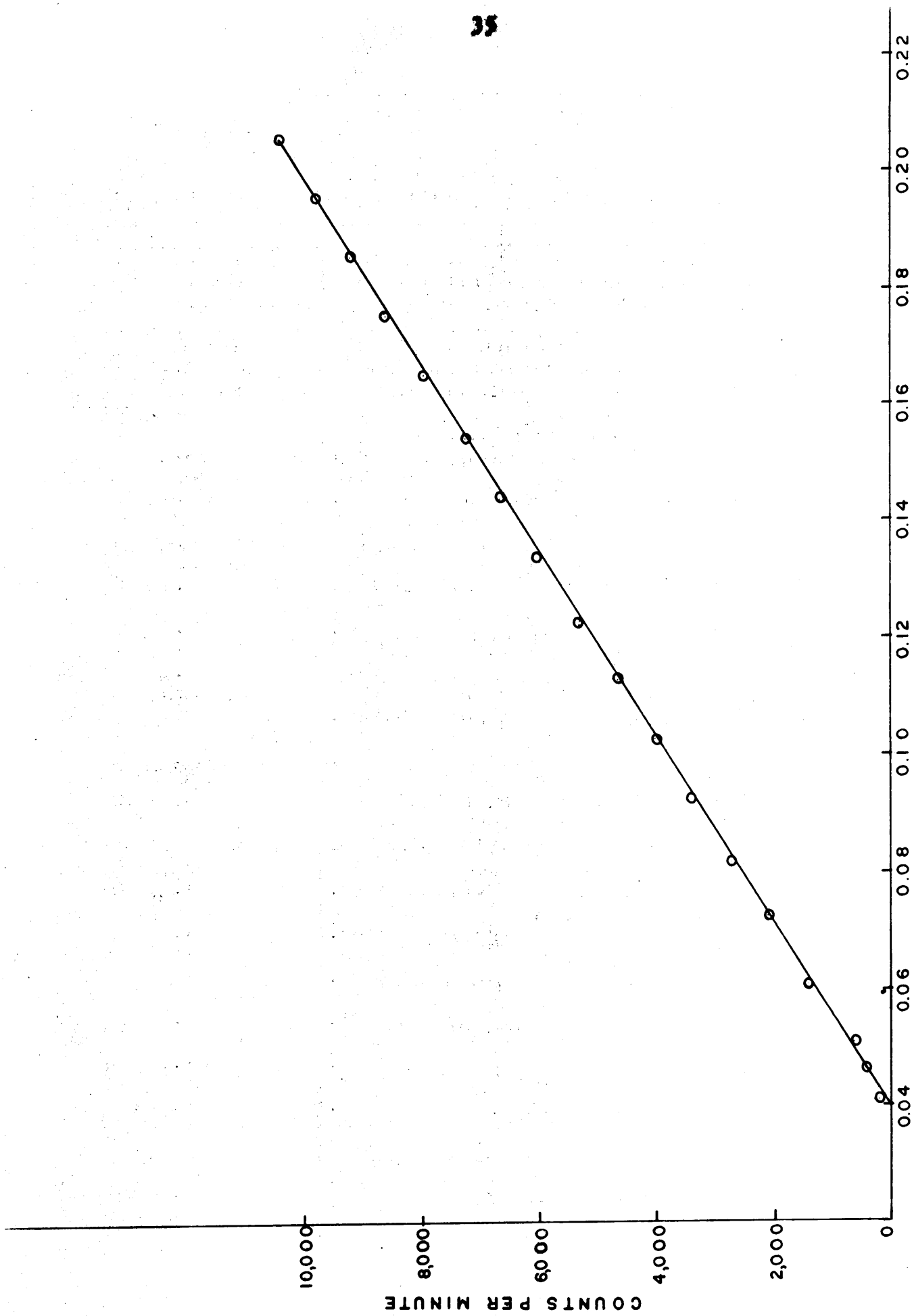


FIG. 8 CALIBRATION OF ELECTRONIC CURRENT INTEGRATOR

## ACCELERATOR OPERATING PROCEDURE

The operation of the accelerator is necessarily complex and the following procedure has been found necessary for successful operation.

The following electronic control and instrumentation equipment should be turned on at least one hour before the machine is put into operation: stabilizer D.C. amplifier, all vacuum tube microammeters, analyzing magnet control equipment, generating voltmeter indicator, electronic current integrator, scintillation detector power supply, all counters, pulse amplifiers and vacuum detection instruments. The spray power supply, generating voltmeter motor, selsyn controls, and stabilizer filament, should remain off until actual operation begins. In addition the cooling water for the analyzing magnet should be turned on, the vacuum system should be evacuated to at least  $1 \times 10^{-5}$  mm of mercury and the pressure system should be pressurized to 150 pounds per square inch with a dew point of at least  $-40^{\circ}\text{C}$ .

After the preliminary operations above, the following step procedure has been adopted:

1. Cycle analyzing magnet approximately ten times by increasing the magnet current to the maximum and then back to zero. This saturation of the

magnet assures operation on the calibrated curve.

2. Adjust the magnet current to correspond to the desired beam energy. This is done by referring to the calibration curve mounted on the control console. The magnet current should be increased gradually to the desired current so that no overshoot occurs. Reducing the magnet current to correct for an overshoot can transfer the magnetization curve to another hysteresis loop.
3. Turn on the belt drive, spray supply filaments, stabilizer filament, generating voltmeter motor, and selsyn power. Allow the belt to run with no spray voltage for several minutes. All the selsyns should be fully counterclockwise. The generating voltmeter and the resistor cascade current meter should indicate a dome potential. This potential is normal and is caused by self-charging of the belt. The equipment in the dome is energized by turning the dome power selsyn clockwise until the microswitch closes. The glow from the ionization tube should be visible through the tank porthole.
4. With the corona needles withdrawn to the limit

and the spray supply control and vernier turned fully counterclockwise, turn on the spray supply high voltage. Very slowly turn the spray control clockwise until the spray current meter indicates a small spray current. The generating voltmeter should indicate an increase in dome potential. It is very important that the spray current is applied slowly; stable operation of the machine is impossible without it. In normal operation, the spray current as shown on the spray current meter should be initially around 25 microamperes, the exact value being dependent upon the humidity and pressure of the gas in the tank. Under no condition should the spray current be increased above 300 microamperes because such currents will puncture the belt. Once the initial spray current is indicated, all further adjustments of the spray current should be made with the vernier control. Increasing the spray current will raise the potential of the dome to the desired value. At this stage the dome potential is not stabilized automatically so it must be regulated manually with the spray vernier control.

5. With one person maintaining the dome potential fairly constant by observing the generating

voltmeter, a second person can adjust the proton source. This is accomplished most efficiently by looking at the color of the glow in the ionization tube. The initial white glow is due to the ionization of the residual gas in the tube. Using the portable controls beside the machine, turn the hydrogen selsyn approximately one turn clockwise. This applies current to the palladium leak. After allowing several minutes for the palladium to heat, one should see the color of the ionization glow turn pink. The vacuum should be monitored during this process and a compromise made between vacuum and amount of hydrogen. Too much hydrogen will quickly destroy the vacuum. Normally a very pink color can be obtained with no serious loss in vacuum. As the temperature inside the dome increases during an extended run, it will be necessary to reduce the amount of hydrogen periodically.

6. The protons formed by the ionization process are expelled from the ionization tube by turning the probe selsyn clockwise. The beam should be visible on the first quartz viewing section after the probe selsyn has been turned clockwise one-half turn.

7. The beam should be focused on the first viewing section by turning the focus selsyn clockwise until a sharp fluorescence is formed. There is some interaction between the probe and focus controls and a compromise must be reached. The quartz viewing section is located at the focal point of the analyzing magnet so if the beam at this point is focused, it will be focused at the target when the quartz is turned so that the beam can enter the magnet.
  
8. With the beam striking the first viewing quartz, the beam stabilizing system can be adjusted. Since the corona needles at this time should be fully withdrawn, the stabilizer plate voltage meter should indicate only a small voltage of perhaps several hundred volts. The stabilizer plate current meter should indicate only a few microamperes. Adjust the stabilizer bias to -22 volts with the bias potentiometer located on the front panel of the stabilizer D.C. amplifier. An external vacuum tube voltmeter must be plugged into the jack provided to indicate the bias voltage. With the D.C. amplifier sensitivity switch set in the sixth position, run the corona needles in until the stabilizer plate

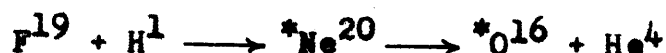


voltage is 1600 volts. The stabilizer current meter should indicate approximately 70 micro-amperes of current. Inserting the corona needles will lower the dome potential so the spray current must be increased to provide this extra current.

9. The beam should pass through the magnet and strike the target when the first viewing quartz is turned out of the path of the beam. If the beam does not go through the magnet, the energy of the beam must be corrected slightly by adjusting the spray vernier control. Once the beam can be seen striking the target, it should be stabilized. The stabilization, in addition to being checked visually, can be seen on the instrument panel. The current integrator registers a very consistent count rate when the beam is stabilized and the balance meters on the stabilizer D.C. amplifier show a slight deflection that varies smoothly as the beam is corrected.
10. Once the beam is stabilized the energy can be increased by increasing only the magnet current. The stabilizer circuit will automatically increase the beam energy through a range of about 200 kilovolts.

## EXPERIMENTAL PROCEDURE

As a measure of the capabilities of the finished accelerator, an investigation was made of the gamma rays produced in the inelastic capture of protons by fluorine, the reaction being the following;



The fluorine nucleus in this reaction captures a proton and forms a compound nucleus which is neon. But the neon nucleus is in an unstable excited state and decays to oxygen with the emission of an alpha particle. The excited states are denoted with an asterisk. The oxygen, however, is also in an excited state and decays by gamma-ray emission to the stable state.

This reaction has been studied quite extensively for the past twenty five years, and though the literature abounds with the results of investigations, four excellent references are Steib,<sup>10</sup> Burcham,<sup>1</sup> Herb,<sup>6</sup> and Hunt.<sup>7</sup>

It has been found that the number of gamma rays produced is a function of the incident energy and at certain energies the production of gamma rays exhibits resonance. These resonances have been studied so

thoroughly that there is general agreement on the energy at which they occur and their natural widths. These known energies and natural widths were used in this investigation as references to determine the resolution of the accelerator.

### Method

A fluorine target was made by applying a slurry of calcium fluoride directly to the target plate. After a 48 hour baking at 150°C to remove all volatile material, the target was mounted in position on the machine.

Following the step procedure above, the energy of the proton beam was stabilized at approximately 300 kev and the target was bombarded with this energy for two minutes. At the start of this interval the scintillation counter and the current integrator counter were started simultaneously and at the end of the interval they were stopped simultaneously. The relative yield was then calculated after the gamma count was corrected for background. The background was determined with the machine operating at approximately 300 kilovolts but with the beam turned off the target. No correction was needed for the current integrator, it being insensitive to any background produced by the accelerator.

The energy of the beam was then increased in 10 kev increments and the target bombarded for two minutes at each energy. The energy was increased by increasing

the magnet current in steps of 0.05 amperes. The relative yield was then calculated for each energy and plotted as a function of the magnet current.

### Results

The results are tabulated in Table 2. and plotted in Fig. 9. The half-maximums of the two resonances occurred at 5.035 amperes and 6.000 amperes. These currents correspond to the well known resonances described by Hunt<sup>7</sup> and occur respectively at 340.4 kev and 483.1 kev.

The differential spectrum for the first resonance, shown in Fig. 10, was obtained graphically from Fig. 9. The observed width at half-maximum corresponds to an energy of 9.6 kev. The resolution was calculated from the well known relationship

$$\Gamma^2 = \Gamma_0^2 - \Gamma_1^2$$

where  $\Gamma_0$  is the observed width and  $\Gamma_1$  is the natural width of the resonance, the most recent value being 2.9 kev.<sup>7</sup> Substituting the observed width and the natural width results in a resolution of 9.1 kev.

Table 2. RELATIVE YIELD AS A FUNCTION OF MAGNET  
CURRENT

<u>Magnet Current</u>	<u>Gamma Counts</u>	<u>Integrator Counts</u>	<u>Relative Yield</u>
4.7689	156	576	0.019
4.8154	160	667	0.023
4.8500	186	688	0.060
4.9022	233	724	0.121
4.9512	207	704	0.088
4.9992	451	690	0.443
5.0565	2759	686	3.80
5.1107	3154	698	4.31
5.1684	3423	703	4.66
5.1960	3453	712	4.65
5.2546	3558	748	4.58
5.3025	3459	722	4.59
5.3500	3388	732	4.43
5.4000	3697	756	4.70
5.4500	3530	738	4.59
5.5000	3727	748	4.79
5.5500	3577	726	4.59
5.5956	3947	910	4.18
5.6486	3722	762	4.70
5.7047	3772	760	4.77
5.7638	4163	840	4.78
5.7996	3911	810	4.66
5.8681	3811	776	4.72
5.9000	3989	845	4.55
5.9622	4004	834	4.62
6.0101	5246	848	6.01
6.0555	5206	865	5.85
6.1215	5565	892	6.08
6.1487	5582	876	6.20
6.2137	5709	914	6.09
6.2966	5628	900	6.10
6.3237	6214	972	6.22
6.3469	6227	981	6.20
6.4078	6364	1126	5.55
6.4765	6876	1174	5.72
6.5184	7722	1226	6.19
6.5564	9208	1366	6.63

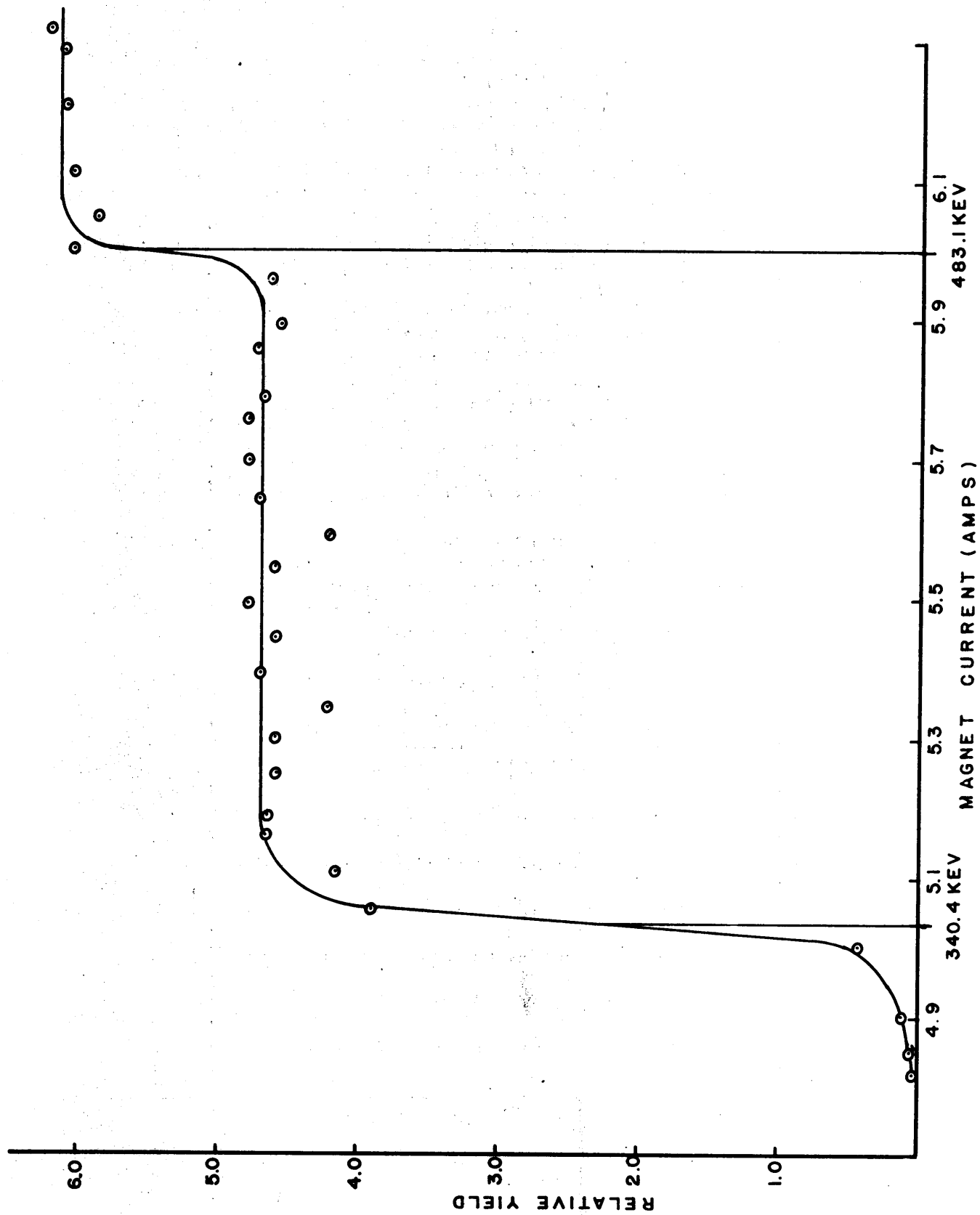


FIG.9 RELATIVE YIELD VS MAGNET CURRENT

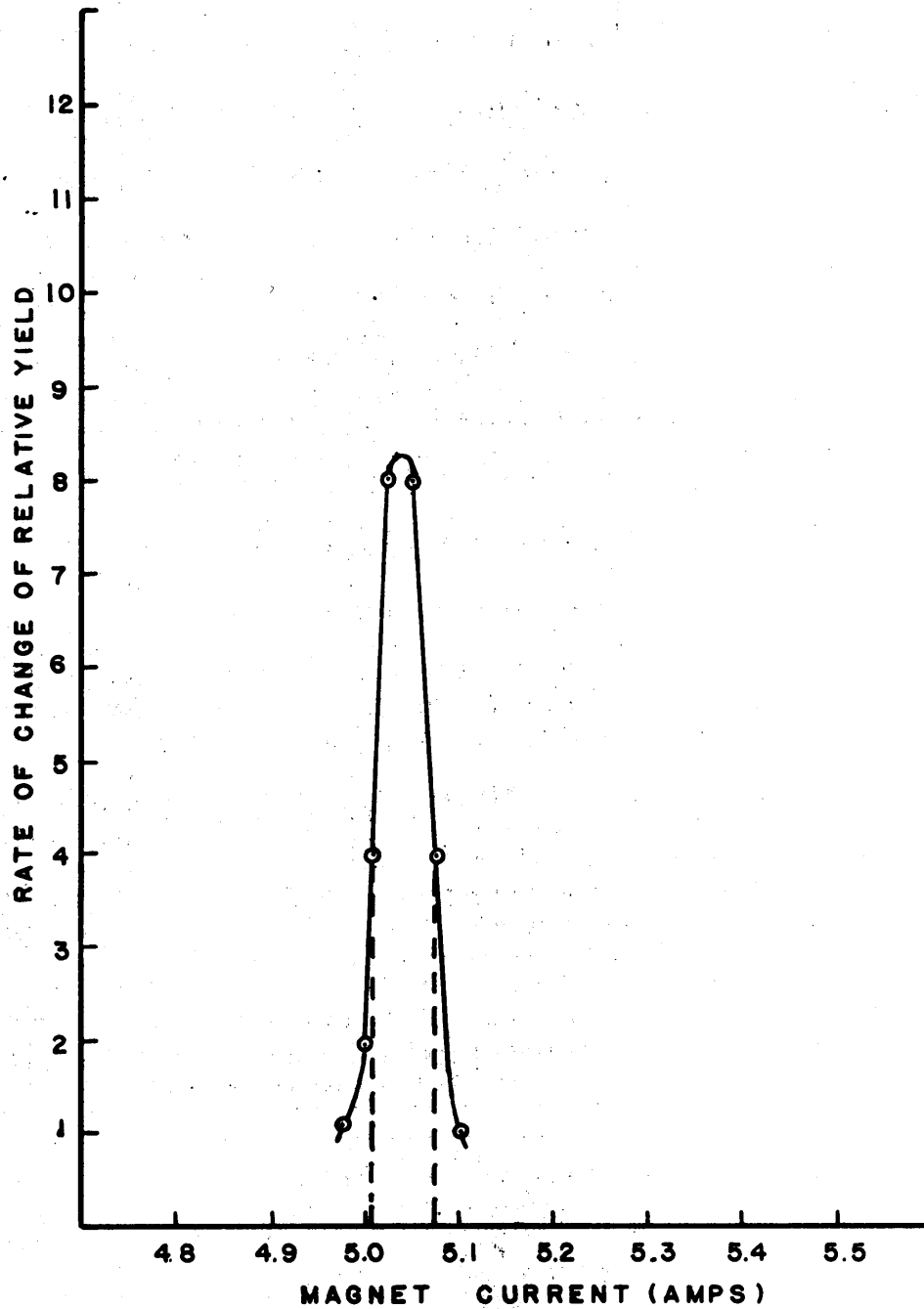


FIG. 10 DIFFERENTIAL SPECTRUM

## DISCUSSION OF RESULTS

The resolution of 9.1 kev at an energy of 340.4 kev represents a deviation in the beam energy of  $\pm 1.4\%$ . This, however, is an upper limit because sufficient points were not obtained on the steeply rising portions of the resonance. Several factors contributed to this limitation. A low beam current of approximately 1 micro-ampere necessitated a wide spacing of the slits in the slit box to obtain sufficient current reaching the target. This spacing decreased the sensitivity of the stabilizer circuit and contributed directly to the resolution figure obtained. A larger beam current would have allowed a much smaller spacing of the slits and a subsequent closer control of the dome potential. Incomplete stabilization of the analyzing magnet current also contributed to the results obtained. At the time the data was taken variations in the magnet current of  $\pm 0.5\%$  could be expected.



## SUMMARY

Though modifications and improvements continue on the Virginia Polytechnic Institute electrostatic accelerator, the basic machine has been completed and put into operation. The emphasis thus far has been upon experiments at energies below 750 kev and no attempt has been made to determine the maximum operating potential.

This work describes the author's contributions to the overall project through the design and construction of many of the electronic control and instrumentation circuits. Through a study of the inelastic collisions of protons with fluorine, a resolution of 9.1 kev was determined.

## ACKNOWLEDGMENTS

The author wishes to express his appreciation to Dr. T.M. Hahn for his guidance and assistance and to  
for his many helpful contributions.  
Such a complex project as an electrostatic accelerator is necessarily a group project and the author wishes to acknowledge the following who contributed in their own way to the overall effort;

. The author wishes to express a special note of appreciation to his wife,  
, for her care in typing the thesis and for her encouragement throughout the project.

## BIBLIOGRAPHY

1. Burcham, W.E. and Devons, S., Proc. Roy. Soc., A173, 555 (1939)
2. Carson, W.E., Voltage Calibration of the V.P.I. Van de Graaff Accelerator Using Thick Targets, M.S. thesis, Virginia Polytechnic Institute, 1958
3. Chramiec, M., Stabilization of the Analyzing Magnet of the V.P.I. Electrostatic Analyzer, M.S. thesis, Virginia Polytechnic Institute, 1958.
4. Elmore, W.C. and Sands, M., Electronics, McGraw Hill Book Company, Inc., p. 405 (1949)
5. Hahn, T.M. and Kern, B.D., Office of Ordnance Research, Final Report for Contract No. DA-33-008-ORD-556, 14 (1954)
6. Herb, R.G., Snowden, S.C., and Sala, O., Phys. Rev., 75, 246 (1949)
7. Hunt, S.E. and Jones, W.M., Phys. Rev., 89, 1283 (1953)
8. Oliver, D.W., The Design and Construction of a Magnetic Analyzer for a Two Million Volt Electrostatic Accelerator, M.S. thesis, Virginia Polytechnic Institute, 1956
9. Rogers, J.S., The Design and Construction of an Ion Source for the V.P.I. 2 Mev Nuclear Accelerator, M.S. thesis, Virginia Polytechnic Institute, 1958
10. Steib, Fowler, and Lauritzen, Phys. Rev., 59, 253 (1941)
11. Watt, B.E., Rev. Sci. Inst., 17, 334 (1946)

**The vita has been removed from  
the scanned document**